Mol. Cells, Vol. 10, No. 6, pp. 712–722

Molecules and Cells

The Na^+–Ca^{2+} Exchanger Is Essential for Embryonic Heart Development in Mice

Chung-Hyun Cho, Sung Sook Kim[1], Myung-jin Jeong[1], Chin O. Lee, and Hee-Sup Shin[1,*]

Department of Life Science, Division of Molecular and Life Science, Pohang University of Science and Technology, Pohang 790-784, Korea;

[1] National Creative Research Initiative Center for Calcium and Learning, Pohang University of Science and Technology, Pohang 790-784, Korea.

(Received on September 14, 2000)

The cardiac Na^+–Ca^{2+} exchanger 1 (NCX1) is thought to be the major calcium extrusion mechanism and to play an important role in the regulation of intracellular calcium in the heart. The Na^+–Ca^{2+} exchanger is particularly abundant in the heart, although it is found in a variety of other tissues. To investigate the role of NCX1, we have generated NCX1-deficient mice. Mice heterozygous for the NCX1 mutation showed no discernable phenotype, grew normally, and were fertile; however, no viable homozygote was observed among 175 offspring obtained from intercrosses of heterozygotes. All the homozygous mutant mice died in utero before E10.5. Morphological analysis indicated that homozygotes of NCX1 mutation at E9.5 died with an underdeveloped heart with a dilated pericardium. Microscopic analysis of these embryos showed myocardial cell loss due to apoptosis. The apoptosis was first observed in E8.5 mutant heart. Areas outside the heart appeared normal in the mutant embryos at E8.5. In contrast, at E9.0, various regions of mutant embryos showed extensive cell loss. These results suggest that mutant embryos die owing to cardiac abnormalities caused by apoptotic cell loss, indicating that NCX1 is essential for normal development of the heart.

Keywords: Ca^{2+} Regulation; Cardiac Abnormalities; Cell Death; Na^+–Ca^{2+} Exchanger; Knockout.

Introduction

Ca^{2+} influx through the L-type Ca^{2+} channel induces excitation of cardiomyocytes. Cardiac relaxation occurs when calcium is removed from the cytosol primarily through the action of two proteins: the sarcoplasmic reticulum Ca^{2+}-ATPase (SERCA) and the sarcolemmal Na^+–Ca^{2+} exchanger (NCX). The exchanger serves as the main calcium extrusion mechanism and plays an important role in the regulation of intracellular calcium in the heart (Blaustein and Lederer, 1999; Bridge *et al*., 1988; Crespo *et al*., 1990). Previous cDNA cloning studies have defined three subtypes of NCX (NCX1, NCX2, and NCX3) that are coded by distinct genes in vertebrates (Li *et al*., 1994; Nicoll *et al*., 1990; 1996). NCX1 is particularly abundant in the heart, although it is expressed in other tissues, whereas NCX2 and NCX3 have been found mainly in brain and skeletal muscle (Li *et al*., 1994; Nicoll *et al*., 1996).

Recent reports have shown that the exchanger may be more important in developing hearts because expression of the NCX1 gene is high in fetal heart but decreases postnatally (Koban *et al*., 1998). In addition, the expression of SERCA and NCX1 is oppositely regulated during heart development and an increase in Ca^{2+} efflux mediated by NCX might compensate for the diminished Ca^{2+} uptake by the SR (Reed *et al*., 2000). Therefore, calcium fluxes via the L-type Ca^{2+} channel and NCX1 might play an important role during cardiac development as well as contraction and relaxation.

Recently, molecular cloning and transgenic technologies have provided the opportunity to manipulate the Na^+–Ca^{2+} exchanger activity *in vivo*. The *in vivo* function of NCX1 has been previously inferred by

* To whom correspondence should be addressed.
Tel: 82-54-279-2291; Fax: 82-54-279-2199
E-mail: shinhs@vision.postech.ac.kr

Abbreviations: ES, embryonic stem; H&E, hematoxylin and eosin; NCX, Na^+–Ca^{2+} exchanger; PCNA, proliferating cell nuclear antigen; SERCA, sarcoplasmic reticulum Ca^{2+}-ATPase; TUNEL, terminal deoxynucleotidyl nick-end labeling; WT, wild type.

overexpression in transgenic mice, in which the overexpression of Na^+–Ca^{2+} exchanger accelerated the decline of intracellular Ca^{2+} during relaxation and strongly affected the SR Ca^{2+} regulation (Adachi-Akahane *et al.*, 1997; Terracciano *et al.*, 1998; Yao *et al.*, 1998). However, the role of NCX1 in other aspects of the heart function is not known. To address this issue, we have generated mice in which the NCX1 gene was ablated by gene targeting. Our results provide evidence for the essential role of the Na^+–Ca^{2+} exchanger in embryonic heart development.

Materials and Methods

Production of knockout mice NCX1-deficient mice were generated by a conventional method (Kim *et al.*, 1997). A mouse genomic DNA library made from 129/sv strain mouse genomic DNA was screened using mouse NCX1 cDNA as a probe (Kim and Lee, 1996). The targeting construct contained a 9.7-kb *Hin*dIII/*Sal*I fragment of genomic DNA with a PGK-neo-poly(A) cassette inserted at the NcoI site located in the first coding exon of the gene and a thymidine kinase gene 3′-flanking the region of homology. This construct disrupted the NCX1 coding sequence after amino acid 247, thereby causing the premature termination. The targeting vector was linearized and electroporated into J1 embryonic stem (ES) cells. The targeted ES cell clones were isolated and injected into C57BL/6J blastocysts and transferred to recipient mice. The resulting chimeras were mated to C57BL/6J female mice to obtain the germline transmission of NCX1 mutation.

Genotyping DNA from ES cells and mouse tail biopsies was genotyped either by Southern blot analysis or by the polymerase chain reaction (PCR). Southern blot analysis was performed using KpnI digests and a 5′-flanking probe that hybridizes to a 12.5-kb and a 10-kb fragment in the case of wild-type (WT) and targeted allele, respectively. Routinely, mouse tail DNA and embryo yolk sac DNA were genotyped by PCR using three primers: a sense primer (5′-ATGCTTCGATTAAGTCTCCCAC-3′) and an antisense primer (5′-TAAAGCCAGGTATAGGCAAAGA-3′) in the exon, and a primer in the PGK sequence (5′-CTGACTAGG GGAGGAGTAGAAG-3′). These reactions amplified a 650-bp fragment from WT allele and a 400-bp fragment from the mutated allele.

Embryo preparation We harvested mouse embryos after natural overnight matings; for staging, fertilization was considered to take place at midnight. Pregnant mothers were killed by cervical dislocation, and the embryos were removed surgically. The tissues were either fixed and embedded in paraffin or processed for DNA extraction.

RNA isolation and RT-PCR Microdissected E8.5–E9.5 mouse embryos were collected, frozen, and stored at −70°C. RT-PCR was carried out using NCX1 primers. Since the NCX1 primers are within exon 2 and do not span an intron, care was taken to treat the RNA with RNase-free DNase to ensure that the PCR fragments were amplified from cDNA and not from genomic DNA (data not shown). PCR amplification of the β-actin gene was carried out using a β-actin primer pair (Promega).

Measurement of heart rate Heart rates were scored microscopically on E9.0 embryos obtained from matings of NCX1 heterozygous. Pregnant females were killed by cervical dislocation. Embryos were removed and placed in a chamber superfused with phosphate-buffered salines at 37°C. Eight WT and four mutant embryos were used to determine heart rates.

Histology and immunohistochemistry Embryos were fixed overnight in 4% buffered formalin and embedded in paraffin. Some sections (5 μm) were used for terminal deoxynucleotidyl nick-end labeling (TUNEL) assay, while others were stained with heamatoxynlin and eosin (H&E) for histological examination. Apoptotic cells were scored using H&E-stained sections by a light microscopic examination under 400× magnification. The number of apoptotic cells was recorded as the number per 100 nuclei (% apoptosis). To confirm the apoptosis, the TUNEL method using an ApopTag *in situ* apoptosis detection kit (Oncor) was performed in each section as described by the manufacturer.

For proliferating cell nuclear antigen (PCNA) staining, sections of embryos were incubated with 1 μg/ml of anti-PCNA antibody at 4°C overnight in PBS with 5% goat serum, 0.2% Tween 20, and 0.1% bovine serum albumin. After incubation, tissue sections were washed and incubated with biotinylated anti-mouse IgG antibody and ABC reagent. Peroxidase was detected with 3,3′-diaminobenzidine.

For measuring the necrotic area, images of embryo sections were magnified (×200) and the necrotic region was outlined separately. The area was calculated with a point-counting procedure using a square lattice grid.

Statistical analysis Results were expressed as mean ± SEM. Statistical comparisons between groups were carried out using an unpaired Student t-test. A level of 0.05 was considered to be indicative of a statistically significant difference.

Results

NCX1 gene disruption is lethal during the early gestational age The construction of the NCX1 gene targeting vector is depicted in Fig. 1A. Targeted ES cells were used to produce chimeric mice and germ-line transmissions were obtained using standard procedures (Kim *et al.*, 1997). Mice heterozygous for the NCX1 gene ($NCX1^{+/-}$) showed no discernable phenotype, grew normally, and were fertile. The genotype was determined within 3 weeks after birth either by Southern blot analysis (Fig. 1B) or by PCR of DNA from tail biopsies. No viable homozygous mouse for the NCX1 mutation ($NCX1^{-/-}$) was observed among the 175 offspring examined in litters from $NCX1^{+/-}$ intercrosses (Table 1), implying embryonic lethality of homozygotes. To assess the consequences of NCX1 mutation on the embryonic development, we determined the geno-

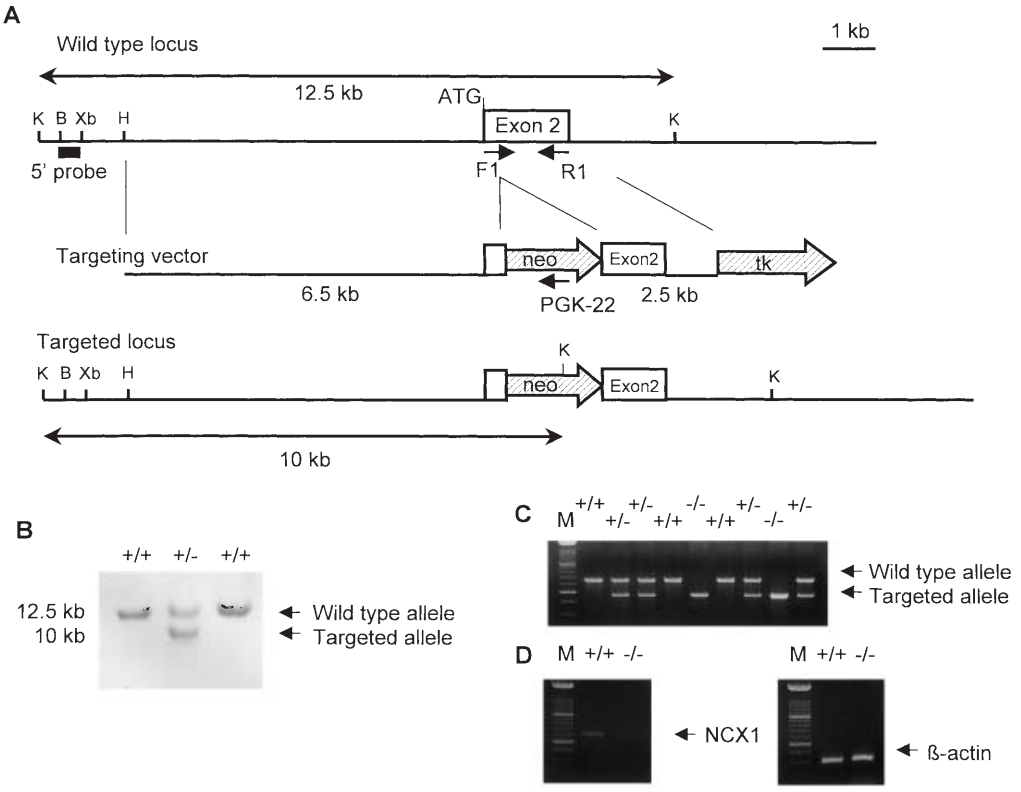

Fig. 1. NCX1 targeting vector and analysis of targeted mutation of NCX1. **A.** Strategy for generation of NCX1 mutation. A partial map of the wild-type mouse NCX1 locus, including exon 2, is shown. The open box is the first coding exon of NCX1, which covers one-third of the total coding region. A PGK-neo^r cassette flanked by a 6.5-kb *Kpn*I-*Nco*I fragment and a 2.5-kb *Xba*I-*Sal*I fragment from the NCX1 genomic DNA clone and a PGK-tk cassette in the targeting vector are illustrated. Digestion with *Kpn*I produces a 10-kb fragment from the targeted allele and a 12.5-kb fragment from the wild-type allele, which can be differentiated by Southern blot analysis with an external probe (closed box). The locations of the external 5′ probe for Southern blotting and primers for PCR genotyping are shown. **B.** Genotyping of KpnI digested genomic DNA from tail biopsies by Southern blot hybridization using a 5′ external probe as shown in **A.** The arrows indicate the 12.5-kb *Kpn*I wild-type allele and 10-kb targeted allele. **C.** PCR genotyping of yolk sac DNA from an E9.5 litter from NCX1$^{+/-}$ parents. The arrows point to the 650-bp DNA fragment amplified from the wild-type allele (with primers F1 and R) and the 450-bp fragment amplified from the targeted-allele (with primers F1 and PGK-22). **D.** RT-PCR analysis of NCX1 gene expression in E9.0 WT and mutant embryos. To check for variation in RNA isolation, PCR amplification of the housekeeping gene ß-myosin was also used. M indicates a 100-bp ladder size marker.

types of embryos from the heterozygous intercrosses by PCR of DNA isolated from yolk sacs and tails at embryonic days between E8.5 and E19.5 (Fig. 1C). No homozygous mutant embryo was identified among 23 embryos obtained from three litters between E10.5 and E19.5 (Table 1); however, homozygous mutants were detected at E8.5 and E9.5 at the predicted Mendelian-inheritance frequency (Table 1). To identify a morphological phenotype associated with an embryonic lethality in NCX1$^{-/-}$ mice, we examined 59 of the E8.5–E9.5 embryos. At E8.5, all embryos appeared normal. NCX1$^{-/-}$ embryos looked identical to WT littermates in size and developmental stage (Figs. 2A and 2B); however, at E9.5, all homozygous mutants were small, less than two-thirds of the normal size range compared with WT littermates (Figs. 2E and 2F). At E9.5, NCX1$^{-/-}$ embryos were necrotic and were in the process of being absorbed. The mutant embryos apparently stopped growing at about E9.0 and thus were smaller than WT embryos at E9.5.

Table 1. Genotypic characterization of offsprings from parents heterozygous at NCX1 locus (NCX$^{+/-}$ × NCX$^{+/-}$).

Age	Genotype of live embryos			Total
	+/+	+/−	−/−	
Postnatal	71 (44)	104 (87)	0 (44)	175
E10.5–E19.5	8 (6)	15 (11)	0 (6)	23
E9.5	11 (9)	15 (18)	10[a] (9)	36
E8.5	6 (6)	10 (11)	7[b] (6)	23

[a] Markedly smaller than littermates.
[b] Morphologically indistinguishable from littermates.
Numbers in parentheses: Number of embryos expected from normal Mendelian inheritance.

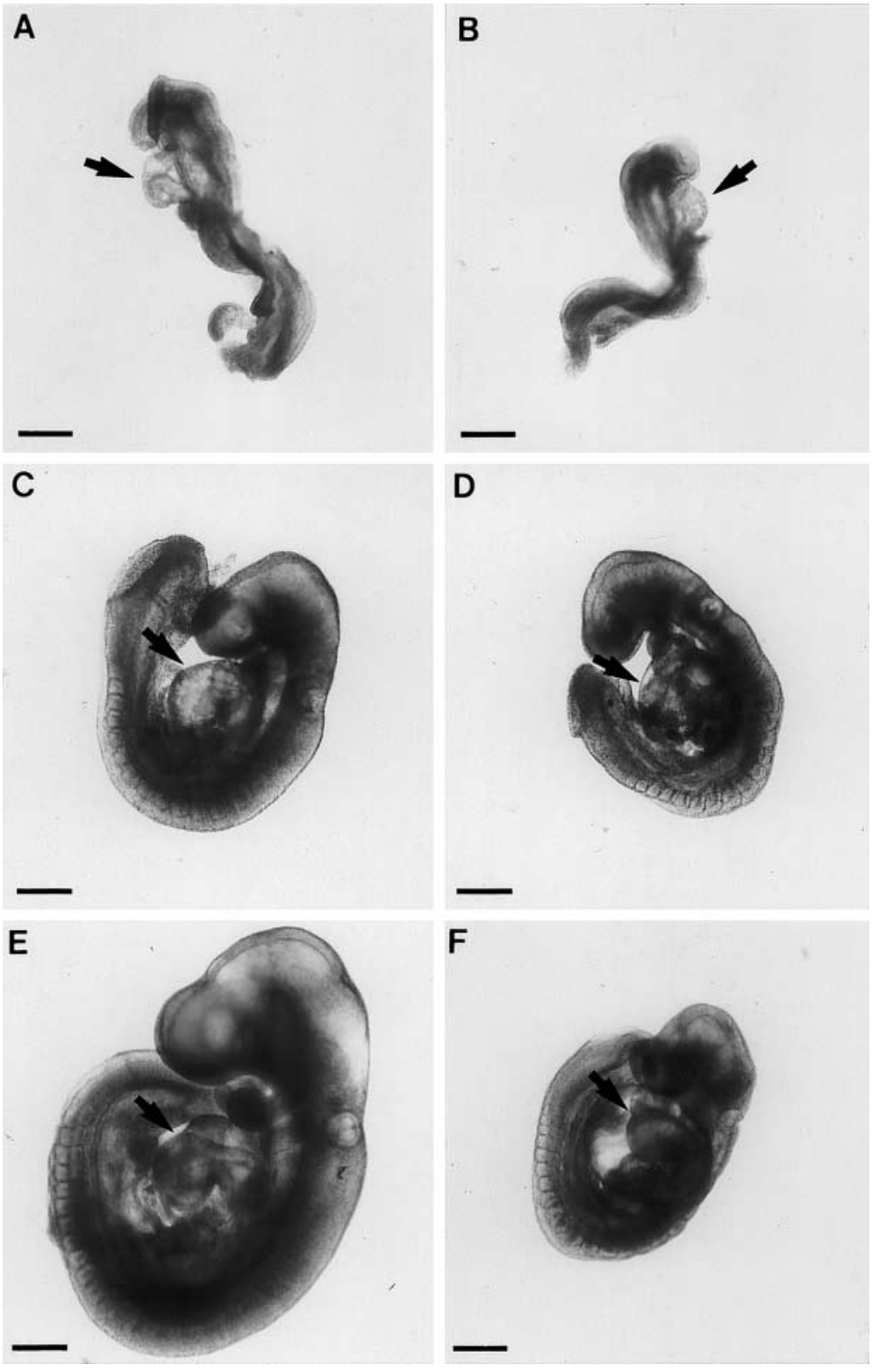

Fig. 2. Morphological analysis of NCX1$^{-/-}$ embryos. Except where indicated, all embryos were produced from mating of NCX1$^{+/-}$ mice. **A** and **B**. No significant difference was detected between WT and mutant embryos at E8.5. **C** and **D**. Comparison of E9.0 WT and NCX1$^{-/-}$ embryos showed the slight size difference in mutant embryos. **E**. By E9.5, WT embryos displayed specified chamber formation and peristaltic contraction. **F**. NCX1$^{-/-}$ embryos, however, were about half the normal size of WT embryos and displayed a severely underdeveloped heart and dilated pericardial sac. However, other structures, including the head and eye, appeared developmentally normal. The arrows indicate the heart. Bar = 50 μm.

To determine that the targeting event resulted in a null mutation, we performed RT-PCR analysis to detect the NCX1 transcripts. Figure 1D shows the NCX1 transcription in E9.0 embryos of WT or heterozygotes. No NCX1 transcripts were found in $NCX1^{-/-}$ embryos, confirming the null mutation of the NCX1 locus.

NCX1 mutant embryos have cardiac abnormalities The most obvious phenotypes in mutant embryos were abnormalities within the heart. Morphological analysis showed that $NCX1^{-/-}$ embryos appeared to develop normally until the cardiac looping stage, but failed to undergo further development. Mutant and WT embryos were alive and grossly indistinguishable at the linear heart tube stage of E8.5 (Figs. 2A and 2B). Their hearts began to form looping morphogenesis and initiated spontaneous contractions in all embryos. At E9.0, in WT embryos, the looped heart was dilated and began to form primitive atrial and ventricular chambers (Fig. 2C). It also exhibited sequential and regular beating with strong atrial contraction preceding ventricular contraction. All mutant embryos at E9.0 were still alive, but appeared slightly delayed in size and appearance compared to WT embryos (Fig. 2D). Although the cardiac looping was successful and atrioventricular demarcation became apparent, the primitive chambers of the mutant embryos were not expanded. The atrial chamber exhibited weak contractions, and the ventricular chamber appeared to vibrate in response to atrial contractions in the $NCX1^{-/-}$ embryos. The heart rates of WT and heterozygous embryos at E9.0 were 53.1 ± 5.9 beats per minute (n = 8), compared to 3.8 ± 1.5 beats per minute for mutants (n = 4, $P < 0.001$, see **Materials and Methods**).

By E9.5, homozygous mutants were unequivocally identifiable by their smaller size (Fig. 2F). Because no embryos of normal appearance and growth were identified as homozygotes, the observed growth retardation phenotype was fully penetrant. No viable homozygous mutants were observed at E9.5, as judged by signs of resorption and the absence of a heart beat. Their anatomical features were similar to those of E9.0 embryos, whereas WT and heterozygous embryos displayed expanded ventricle and atrium showing regular peristaltic beats and blood circulation (Fig. 2E). Around E9.5, the homozygous mutants also exhibited a severely dilated pericardial sac (Fig. 2F), which was also seen in embryos that died from cardiac defects as a result of other mutations (Lin *et al.*, 1997; Riley *et al.*, 1998). At E10.5, no mutant embryos were identified; instead bloody and largely empty implantation sites showed that the mutant embryos had been resorbed (data not shown).

NCX1 mutants' lethality results from the aborted development of the heart Consistent with morphological assessment, histological analysis of homozygous mutant embryos on E8.5 showed no significant differences from normal littermates (Figs. 3A and 3B). The heart tube was regularly organized with a single myocardium and the neural tube remained open.

At E9.0, the looped heart of WT and heterozygous embryos began to specify itself to form primitive atrial and ventricular chambers, in which the myocardium and endocardium were evident and the epicardium, the single layer surrounding the heart, was organized (Fig. 3C). The blood cells were detected in the ventricular cavity. However, in the mutant heart of E9.0 embryos, the walls of the atrial and ventricular chambers were still thin in what should be a dense layer at this stage (Fig. 3D). Although the atrioventricular demarcation was present in the mutant, the endocardial cushions did not form. Blood cells were also seen in the mutant heart, but very few were present in the heart, indicating that circulation was impaired. By E9.5, the common atrium and ventricle became distinct as valves formed and the ventricular myocardium proliferated to form trabeculae in a normal heart (Fig. 3E). In the mutant heart of E9.5 embryos, however, the cardiomyocytes within the ventricular wall were arranged irregularly, inner trabeculation was poorly developed, and the myocardium was markedly thinner than that of the WT control (Fig. 3F). The endocardial lining surrounding the myocardial trabeculation of the mutant hearts was also less complex than that of WT hearts.

The examination of other organs showed that the development of the neural tube, somites, the head fold, and limb buds of homozygous mutant embryos were developmentally normal, but small. In addition, there was no evidence for hematopoietic failure in the NCX1 mutant mice (data not shown).

Apoptotic loss of cardiomyocytes interferes with the development of the heart in $NCX^{-/-}$ embryos A higher-power view of the myocardium of E8.5–E9.5 mutant embryos showed the presence of subcellular bodies in cardiomyocytes (Fig. 4). While no apparent difference in the frequency of cell death was found between the mutant and WT embryos at E8.5, high-power images of histological sections revealed that in E9.0 $NCX1^{-/-}$ embryos many degenerating cells were observed: in various regions, including the neural tube and interstitial cells, grouped deaths were detected (Fig. 5). They showed characteristic features of necrosis, such as plasma membrane disintegration, leakage of cell contents, and grouped deaths (Haunstetter and Izumo, 1998; van den Hoff *et al.*, 2000). The necrotic area was 7.5 ± 1.9% in E9.0 mutant embryos (n = 3) and progressively more increased to 15.9 ± 0.9% in E9.5 mutant embryos compared to WT embryos (n = 3, $P < 0.01$, Table 2), indicating homozygotes of NCX1 mutation were in the process of dying during E9.0.

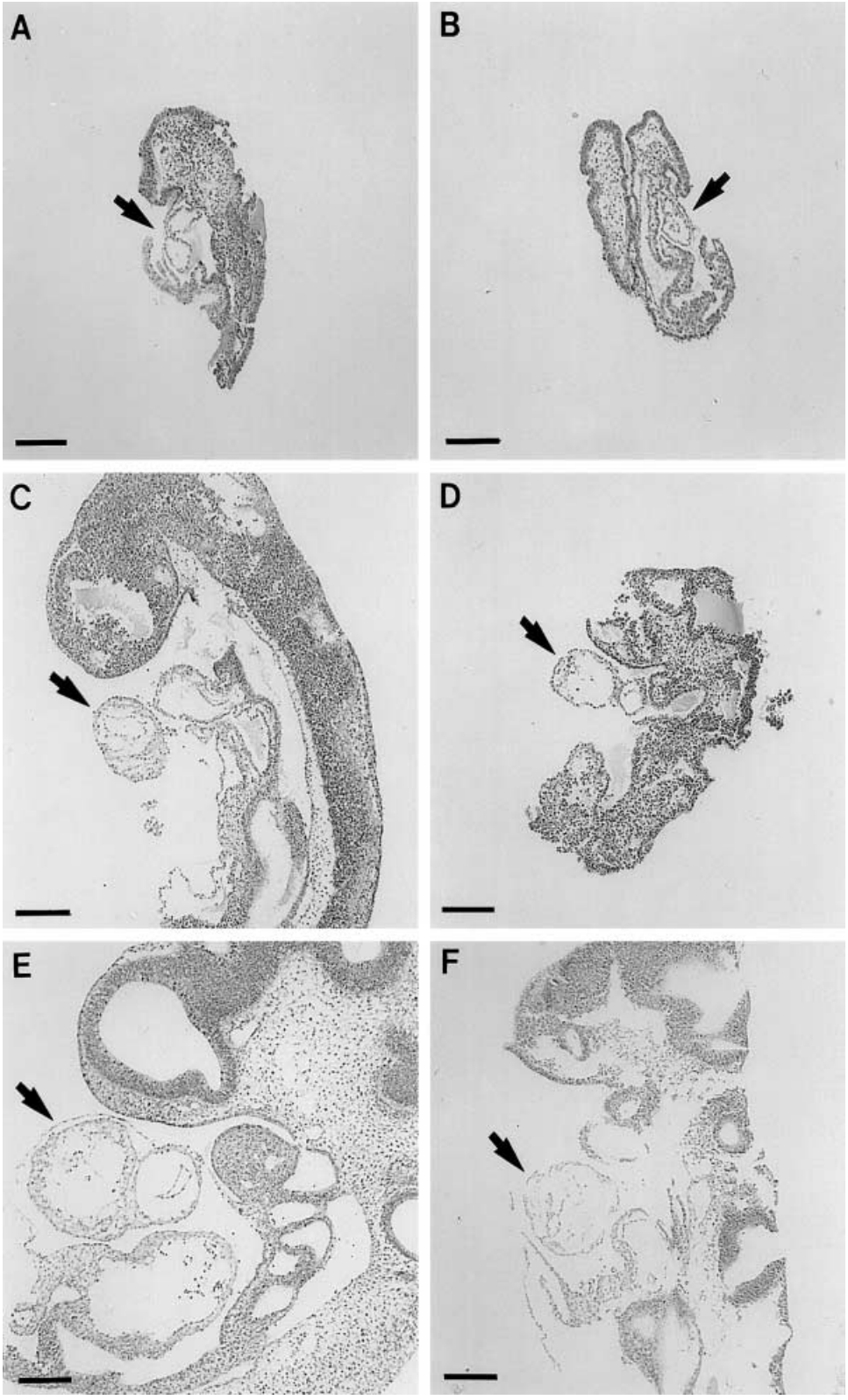

Fig. 3. Histological analysis of WT and NCX$^{-/-}$ embryos at E8.5-E9.5. **A** and **B**. Sagittal sections of WT and NCX1$^{-/-}$ embryos at E8.5. Serial sections displayed the integrity of a looped heart tube and no significant difference was detected. **C** and **D**. Sections of E9.0 WT and mutant embryos. Mutant heart was slightly underdeveloped with thin ventricular walls. **E** and **F**. Sections of E9.5 WT and mutant embryos. Mutant embryos displayed markedly smaller and severely disorganized heart structures than WT embryos. The arrows indicate the heart. Bar = 25 μm.

The observed deficiency in development and subcellular bodies suggested that many cells in the NCX1$^{-/-}$ embryos had undergone cell deaths. To determine the cause of abnormal development in the mutant hearts, we examined whether apoptosis or alteration in cell proliferation occurred in NCX1$^{-/-}$ embryos. Apoptotic cells could be identified in H&E sections as cells with fragmented nuclei and condensed cytoplasm or as small aggregates of nuclear and/or cytoplasmic fragments replacing on cells (Gavrieli *et al*., 1992; van den Hoff *et al*., 2000). Whereas apoptotic cells were infrequently found in the WT myocardium, apoptotic cells were frequently detected in E8.5–E9.5 mutant hearts (Fig. 4). To assess the extent of apoptosis in NCX1$^{-/-}$ hearts, the numbers of apoptotic cells were scored microscopically. Table 2 gives the proportion of the number of apoptotic cells to the total number of heart cells. The values of % apoptosis in E8.5, E9.0, and E9.5 mutant hearts were 9.8 ± 0.8%, 10.5 ± 1.3%, and 12.6 ± 0.5%, respectively. These values of the mutant embryos were significantly higher than the 3.0 ± 0.8%, 2.8 ± 0.6%, and 1.7 ± 0.2% of WT embryos, respectively ($P < 0.05$), indicating the increased loss of myocardial cells. Apoptotic cell deaths were also confirmed by the TUNEL analysis (Fig. 6).

To investigate whether the NCX1$^{-/-}$ embryos exhibited inappropriate proliferation, we performed the PCNA analysis with tissue sections from E8.5–E9.5 embryos. No significant difference in proliferation was detected between WT and mutant embryos. In tissue sections from WT embryos, 10.2 ± 2.5% of the nuclei in the heart were stained positive (n = 3), while 11.8 ± 1.8% were positive in the NCX1$^{-/-}$ embryos (n = 3). This indicates that NCX1 deficiency did not affect the proliferation of cardiac myocytes and that NCX1-deficient embryos underwent net cell loss due exclusively to excessive apoptosis, which began in the heart at E8.5.

Discussion

The cardiac NCX plays a primary role in Ca^{2+} efflux and is important in regulating the intracellular Ca^{2+} and cardiac contractility (Lee, 1985). Although its expression is widespread, its dominant expression in the heart may imply a special role in the function of the tissue (Li *et al*., 1994; Nicoll *et al*., 1990; 1996). The objectives of this study were to develop NCX1-deficient mice and to analyze the phenotype to better understand its functional role in the heart. In the present study, we showed that NCX1 played an essential role in embryo development in mice. The absence of NCX1 was lethal to the embryo at approximately E9.0 as a result of cardiac abnormalities. Cardiac development was severely compromised by myocardial cell loss.

The most noticeable defect was detected within the heart. The heart is the first organ to form during embryogenesis and the proper function of the heart is a prerequisite for embryonic survival (Kaufman, 1992). In mice, by E8.0, as the embryo folded laterally, bilateral heart primordia migrate to the ventral midline and fuse with each other to form a single heart tube, a primitive heart tube, and then begin to contract irregularly. Subsequently, the heart tube undergoes looping and septation. By E9.0, the atrial portion shifts dorsally and to the left, and the boundaries between the common atrium, the primitive ventricle (the future left ventricle), and the bulbus cordis (the future right ventricle) become prominent, and the primitive atria and ventricles beat regularly and powerfully (Kaufman, 1992). In the absence of NCX1, the formation of the primitive heart tube and cardiac looping appeared to occur normally, suggesting that NCX1 was unlikely to be required for the development of the primitive heart tube. On the other hand, there were defects in the specification and growth of the primitive chambers, accompanied by irregular and impaired contraction in mutant embryos. Morphological abnormalities of the heart may or may not be the cause of embryonic lethality of the NCX1$^{-/-}$ mice, because NCX1 is known to be expressed in most other cells in adults and may take part in as yet unknown functions. However, evidence indicates that the expression of NCX1 is restricted to the murine embryonic heart until E11 (Koushik *et al*., 1999). Histological analysis also revealed cardiomyopathic changes with hypoplasia in NCX1$^{-/-}$ embryos. Taken together, these data suggest that the NCX1 deficiency might primarily damage the embryonic heart and the observed growth arrest of NCX1$^{-/-}$ embryos was likely due to the dysfunction of the abnormal heart.

It was revealed that the cardiac defect of the NCX1$^{-/-}$ embryo was associated with the increased apoptosis of cardiomyocytes. Apoptosis is a type of cell death in which the cell actively participates in its own destruction by utilizing a set of genetically programmed responses and a complex network of enzymes (Trump *et al*., 1997). During cardiac development, programmed cell death is suggested to be of importance in the integrity of the heart structure (James *et al*., 1996; Taketa *et al*., 1996); however, inappropriate apoptosis is suggested to be a possible mechanism in the pathogenesis of the heart (Sabbah, 2000). The heart of NCX1-deficient embryos showed disorganization of the myocardium and abundant apoptotic cell deaths. Apoptosis began at the E8.5 stages of development and was prominent in the primitive ventricular cells of E9.5 mutant embryos. Although other forms of cell death might also have occurred, our data suggested that the apoptosis contributed to the loss and disorganization of cardiomyocytes in the NCX1-deficient heart. The observed apoptosis

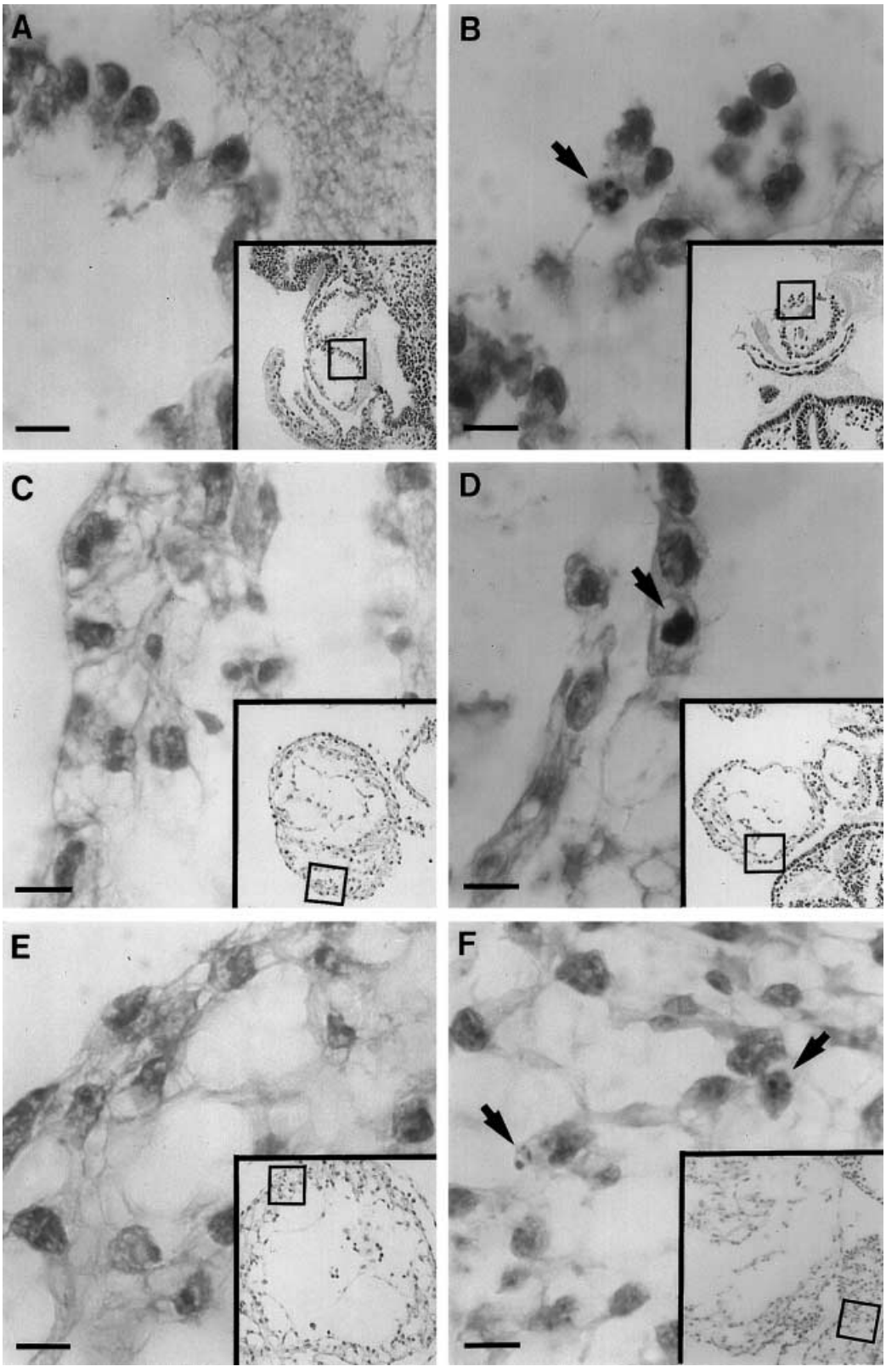

Fig. 4. Apoptotic cell deaths of E8.5–E9.5 embryonic hearts. **A**, **C,** and **E**. High power view of WT cardiomyocytes at E8.5, E9.0, and E9.5, respectively, which is indicated on the hearts as squares (inset). WT heart showed a regularly arrayed myocardium and normal development to specified ventricular and atrial chambers. **B**, **D**, and **F**. $NCX1^{-/-}$ myocardium at E8.5, E9.0, and E9.5, respectively, which showed apoptotic cells. Mutant heart appeared relatively thin and have a disorganized myocardium and abnormal development (inset). The arrows indicate the apoptotic cells showing characteristic features of nuclear fragmentation and condensation. Bar = 1 μm.

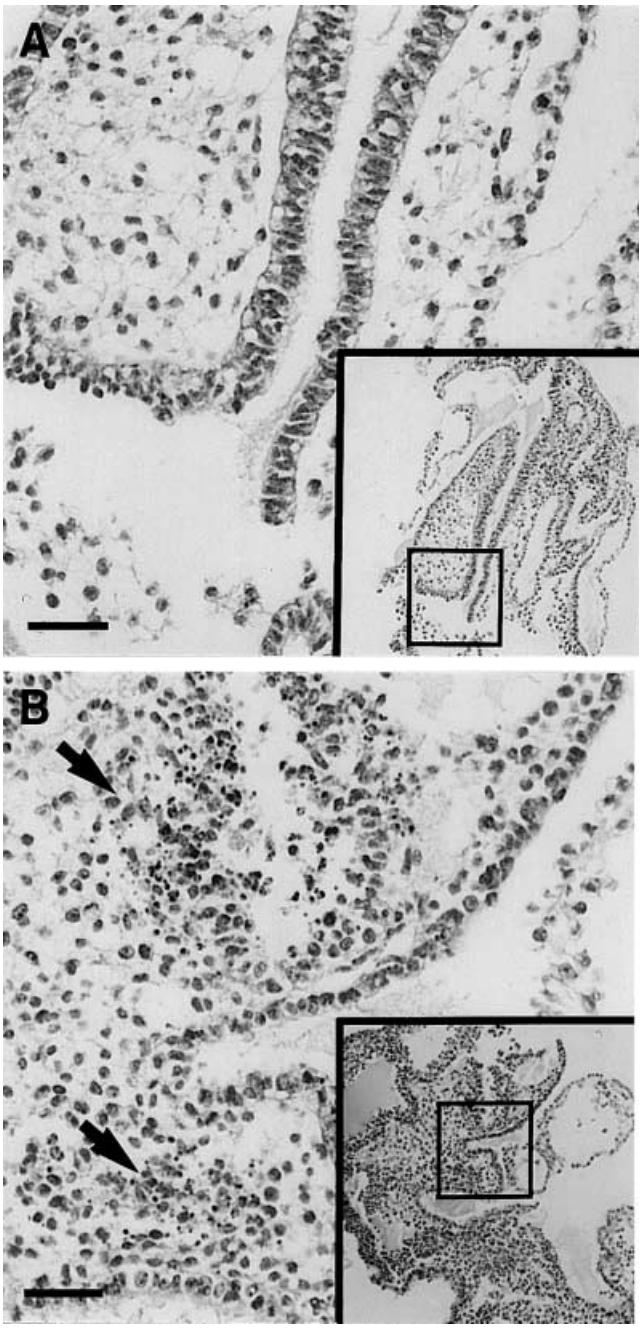

Fig. 5. Necrotic cell deaths in NCX1$^{-/-}$ embryos. **A.** High-power view of the area indicated in E8.5 mutant embryo (inset). No necrotic or degenerating cell was detected in nonmyocytic cells. **B.** High-power view of the area indicated in the E9.0 mutant embryo (inset). Progressive degenerating or necrotic cells were observed in head folds and limb buds. The arrows indicate the necrotic areas. Bar = 1 μm.

either might be a direct effect of NCX1 deficiency in the cells or could be secondary to decreased cardiac function. The former explanation appears more plausible, as the expression of NCX1 was restricted to the heart at E8.5 (Koushik *et al.*, 1999) and apoptotic cells were detected in the mutant hearts at this stage, even though the normal development including the heart and other organs had occurred up to this stage.

Table 2. Apoptotic and necrotic indices of embryos during development.

	% of apoptotic cells[a]		% of necrotic areas[b]	
	(+/+)	(−/−)	(+/+)	(−/−)
E8.5	3.0 ± 0.8	9.8 ± 0.8[c]	0.0 ± 0.0	0.0 ± 0.0
E9.0	2.8 ± 0.6	10.5 ± 1.3[c]	0.0 ± 0.0	7.5 ± 1.9[d]
E9.5	1.7 ± 0.2	12.6 ± 0.5[c]	0.0 ± 0.0	15.9 ± 0.9[d]

[a] The number of apoptotic cells to the total heart cells.
[b] The necrotic area to the total embryo area.
[c] $P < 0.05$ vs WT control.
[d] $P < 0.01$, necrotic area of the mutant embryos at E9.0 vs at E9.5.
Results are expressed as mean ± SEM (n = 3 for all groups).

In addition to cardiac defects, the population of dead cells with a disrupted cell membrane in the neural tube and other organs were first detected from E9.0 mutant embryos and progressively increased at E9.5. This form of cell death is a characteristic feature of necrosis in which cell death does not involve suicide mechanisms and shows immediate loss or rupture of the plasma membrane (Takashi and Ashraf, 2000; Trump *et al.*, 1997). Because the organization and formation of tissues into organs at this stage (E8.5–E10.5) require efficient vascular delivery of nutrients and removal of waste products, an impaired cardiac function might cause the nutrient deficiency in embryos. Therefore, it is possible that the delayed morphogenesis of the heart from apoptotic loss of cardiomyocytes and the accompanied functional defect was most likely responsible for the necrotic or apoptotic cells in other tissues. This could result in embryonic lethality.

In mature cardiac myocytes, excitation–contraction coupling is mediated by Ca^{2+} release from the sarcoplasmic reticulum, which is triggered by the Ca^{2+} entry through the transsarcolemmal Ca^{2+} channels (McDonald *et al.*, 1994); however, during early embryonic development, cardiac excitation and contraction are more dependent on the transsarcolemmal Ca^{2+} influx because of immature Na^{+} channels and Ca^{2+} regulatory properties of SR (Davies *et al.*, 1996; Park *et al.*, 1998). The functional L-type Ca^{2+} channel current is detected in E9.5 embryos and is assumed to be expressed in early developmental stage (Liu *et al.*, 1999), which is in agreement with the fact that the primitive mouse heart began to beat rhythmically at E9.0. Thus, Ca^{2+} removal is more important for relaxation in a developing heart than in an adult heart. Without the Ca^{2+} extrusion mechanism, cardiac myocytes may become overloaded with Ca^{2+}, which might be the cause of apoptotic cell death (Nicotera and Orrenius, 1998). These reports and the results of the present study

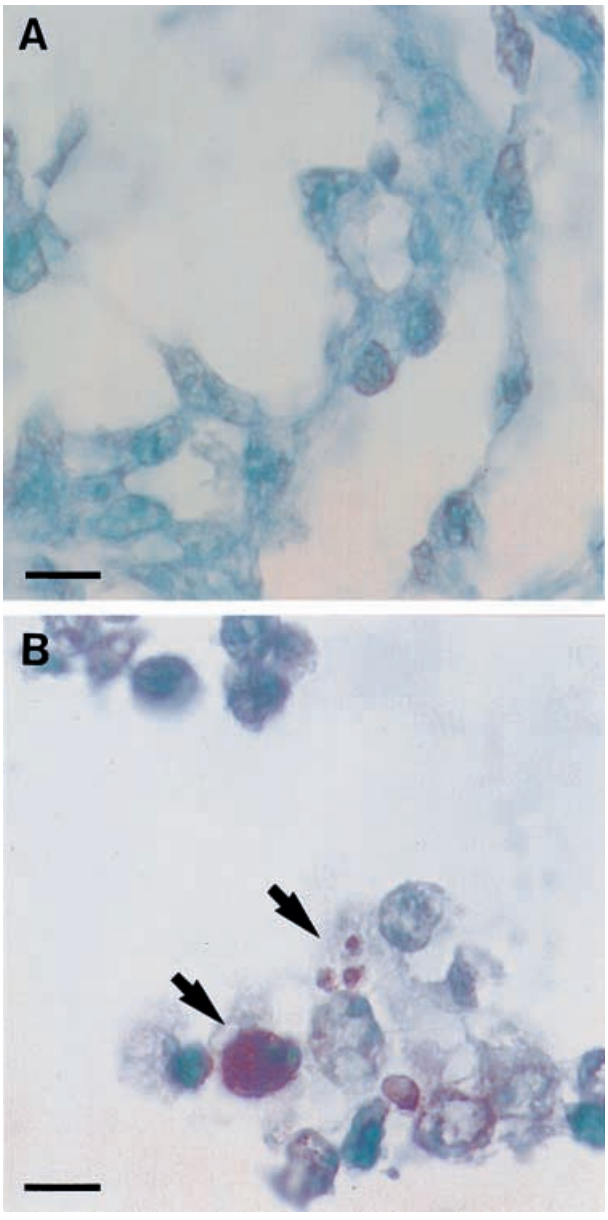

Fig. 6. Apoptotic cell deaths in the NCX1$^{-/-}$ myocardium. **A** and **B**. TUNEL assay of E8.5 WT and mutant myocardium. The arrows indicate the TUNEL-positive cells. Bar = 1 μm.

suggest that Na^+–Ca^{2+} exchange might be essential for the regulation of intracellular Ca^{2+} levels in developing hearts.

In summary, the present study shows that (1) the embryos deficient in NCX1 did not survive, (2) the hearts of the embryos had abnormal development, and (3) the cells of the hearts were apoptotic. This indicates that NCX1 plays a critical role in normal heart development.

Acknowledgments We thank K. Jun, D. Kim, and Y. Namkung for superb technical advice and assistance on gene targeting, and M. P. Kong for blastocyst injection and animal care. This work is supported by a grant from the National Creative Research Initiative Program, Korea, and a grant from the Korea Science and Engineering Foundation (98-0403-0801).

References

Adachi-Akahane, S., Lu, L., Li, Z., Frank, J. S., Philipson, K. D., and Morad, M. (1997) Calcium signaling in transgenic mice overexpressing cardiac Na^+–Ca^{2+} exchanger. *J. Gen. Physiol.* **109**, 717–729.

Blaustein, M. P. and Lederer, W. J. (1999) Sodium/calcium exchange: its physiological implications. *Physiol. Rev.* **79**, 763–854.

Bridge, J. H. B., Spitzer, K. W., and Ershler, P. R. (1988) Relaxation of isolated ventricular cardiomyocytes by a voltage-dependent process. *Science* **241**, 823–825.

Crespo, L. M., Grantham, C. J., and Cannell, M. B. (1990) Kinetics, stoichiometry and role of the Na-Ca exchange mechanism in isolated cardiac myocytes. *Nature* **345**, 618–621.

Davies, M. P., An, R. H., Doevendans, P., Kubalak, S., Chien, K. R., and Kass, R. (1996) Developmental changes in ionic channel activity in the embryonic murine heart. *Circ. Res.* **78**, 15–25.

Gavrieli, Y., Sherman, Y., and Ben-Sasson, S. A. (1992) Identification of programmed cell death in situ via specific labeling of nuclear DNA fragmentation. *J. Cell. Biol.* **119**, 493–501.

Haunstetter, A. and Izumo, S. (1998) Apoptosis: basic mechanisms and implications for cardiovascular disease. *Circ. Res.* **82**, 1111–1129.

James, T. N., St. Martin, E., Willis, P. W. III., and Lohr, T. O. (1996) Apoptosis as a possible cause of gradual development of complete heart block and fatal arrhythmias associated with absence of the AV nose, sinus node, and internodal pathway. *Circulation* **93**, 1424–1438.

Kaufman, M. (1992) *The Atlas of Mouse Development*, Academic, London.

Kim, D., Jun, K. S., Lee, S. B., Kang, N. G., Min, D. S., Kim, Y. H., Ryu, S. H., Suh, P. G., and Shin, H. S. (1997) Phospholipase C isozymes selectively couple to specific neurotransmitter receptors. *Nature* **389**, 290–293.

Kim, I. and Lee, C. O. (1996) Cloning of the mouse cardiac Na^+–Ca^{2+} exchanger and functional expression in Xenopus oocytes. *Ann. NY Acad. Sci.* **779**, 126–128.

Koban, M. U., Moorman, A. F. M., Holtz, J., Yacoub, M. H., and Boheler, K. R. (1998) Expressional analysis of the cardiac Na–Ca exchanger in rat development and senescence. *Cardiovasc. Res.* **37**, 405–423.

Koushik, S. V., Bundy, J., and Conway, S. J. (1999) Sodium-calcium exchanger is initially expressed in a heart-restricted pattern within the early mouse embryo. *Mech. Dev.* **88**, 119–122.

Lee, C. O. (1985) 200 years of digitalis: the emerging central role of the sodium ion in the control of cardiac force. *Am. J. Physiol.* **249**, C367–378.

Li, Z., Matuoka, S., Hryshko, L. V., Nicoll, D. A., Bersohn, M. M., and Burke, E. P. (1994) Cloning of the NCX2 isoform of the plasma membrane Na^+–Ca^{2+} exchanger. *J. Biol. Chem.* **269**, 17,434–17,439.

Lin, Q., Schwarz, J., Bucana, C., and Olson, E. N. (1997) Control of mouse morphogenesis and myogenesis by transcription factor MEF2C. *Science* **276**, 1404–1407.

Liu, W., Yashui, K., Arai, A., Kamiya, K., Cheng, J., Kodama, I., and Toyama, J. (1999) β-Adrenergic mod-

ulation of L-type Ca^{2+}-channel currents in early-stage embryonic mouse heart. *Am. J. Physiol.* **276**, H608–H613.

McDonald, T. F., Pelzer, S., Trautwein, W., and Pelzer, D. J. (1994) Regulation and modulation of calcium channels in cardiac, skeletal, and smooth muscle cells. *Physiol. Rev.* **74**, 365–507.

Nicoll, D. A., Longoni, S., and Philipson, K. D. (1990) Molecular cloning and functional expression of the cardiac sarcolemmal Na^{+}–Ca^{2+} exchanger. *Science* **250**, 562–565.

Nicoll, D. A., Quednau, B. D., Qui, Z. Y., Xia, Y., Lusis, A. J., and Philipson, K. D. (1996) Cloning of a third mammalian Na^{+}–Ca^{2+} exchanger, NCX3. *J. Biol. Chem.* **271**, 24,914–24,921.

Nicotera, P. and Orrenius, S. (1998) The role of calcium in apoptosis. *Cell Calcium* **23**, 173–180.

Park, M. Y., Park, W. J., and Kim, D. H. (1998) Expression of excitation–contraction coupling proteins during muscle differentiation. *Mol. Cells* **8**, 513–517.

Reed, T. D., Babu, G. J., Ji, Y., Zilberman, A., Ver Heyen, M., Wuytack, F., and Periasamy, M. (2000) The expression of SR calcium transport ATPase and the Na^{+}–Ca^{2+} exchanger are antithetically regulated during mouse cardiac development and in hypo/hyperthyroidism. *J. Mol. Cell. Cardiol.* **32**, 453–464.

Riley, P., Anson-Cartwright, L., and Cross, J. C. (1998) The Hand1 bHLH transcription factor is essential for placentation and cardiac morphogenesis. *Nature Genet.* **18**, 271–275.

Sabbah, H. N. (2000) Apoptotic cell death in heart failure. *Cardiovasc. Res.* **45**, 704–712.

Takashi, E. and Ashraf, M. (2000) Pathologic assessment of myocardial cell necrosis and apoptosis after ischemia and reperfusion with molecular and morphological markers. *J. Mol. Cell. Cardiol.* **32**, 209–224.

Takeda, K., Yu, Z. X., Nishikawa, T., Tanaka, M., Hosoda, S., Ferrans, V. J., and Kasajima, T. (1996) Apoptosis and DNA fragmentation in the bulbus cordis of the developing rat heart. *J. Mol. Cell. Cardiol.* **28**, 209–215.

Terracciano, C. M., Souza, A. I., Philipson, K. D., and MacLeod, K. T. (1998) Na^{+}–Ca^{2+} exchange and sarcoplasmic reticular Ca^{2+} regulation in ventricular myocytes from transgenic mice overexpression the Na^{+}–Ca^{2+} exchanger. *J. Physiol Lond.* **512**, 651–667.

Trump, B. F., Berezesky, I. K., Chang, S. H., and Phelps, P. C. (1997) The pathways of cell death: oncosis, apoptosis and necrosis. *Toxicol. Pathol.* **25**, 82–88.

Yao, A., Su, Z., Nonaka, A., Zubair, I., Lu, L., Philipson, K. D., and Morad, M. (1998) Effects of overexpression of the Na^{+}–Ca^{2+} exchanger on $[Ca^{2+}]_i$ transients in murine ventricular myocytes. *Circ. Res.* **82**, 657–665.

van den Hoff, M. J. B., van den Eijnde, S. M., Viragh, S., and Moorman, A. F. M. (2000) Programmed cell death in the developing heart. *Cardiovasc. Res.* **45**, 603–620.